Supplementary Information

A clean transfer approach to prepare centimetre-scale black phosphorus crystalline multilayers on silicon substrates for field-effect transistors

Yuqian Zhao[1‡], Jianfeng Mao[1‡], Zehan Wu[1], Weng Fu Io[1], Sin -Yi Pang[1], Yifei Zhao[1], Jianhua Hao[1*]

[1] *Department of Applied Physics, The Hong Kong Polytechnic University, Hong Kong, P. R. China.*

[‡]Y. Zhao and J. Mao contributed equally to this work.

*Corresponding author.

E-mail address: jh.hao@polyu.edu.hk

Surface energies of different surfaces

The surface energies were evaluated by measuring the contact angles of EG and glycerol, employing the Owen-Wendt method (1) and Young's equation (2). Equation (3) was derived by combining equations (1) and (2) to calculate the surface energies.

$$\gamma_{AL} = \gamma_A + \gamma_{LV} - 2(\gamma_A^d \gamma_{LV}^d)^{1/2} - 2(\gamma_A^p \gamma_{LV}^p)^{1/2} \tag{1}$$

$$\gamma_A = \gamma_{LV} \cos(\theta) + \gamma_{AL} \tag{2}$$

$$\gamma_{LV}(\cos(\theta) + 1) = 2(\gamma_A^d \gamma_{LV}^d)^{1/2} + 2(\gamma_A^p \gamma_{LV}^p)^{1/2} \tag{3}$$

Here, γ_{AL} represents the surface energy between used liquid and solid surface A. γ_L and γ_A are the surface energies of the liquid and solid, respectively. The terms d and p correspond to the dispersion and polar components, respectively. The contact angle of the liquid on the substrate is denoted as θ. Supplementary Table 1 provides a list of the surface energies of the tested liquids, namely EG and glycerol.

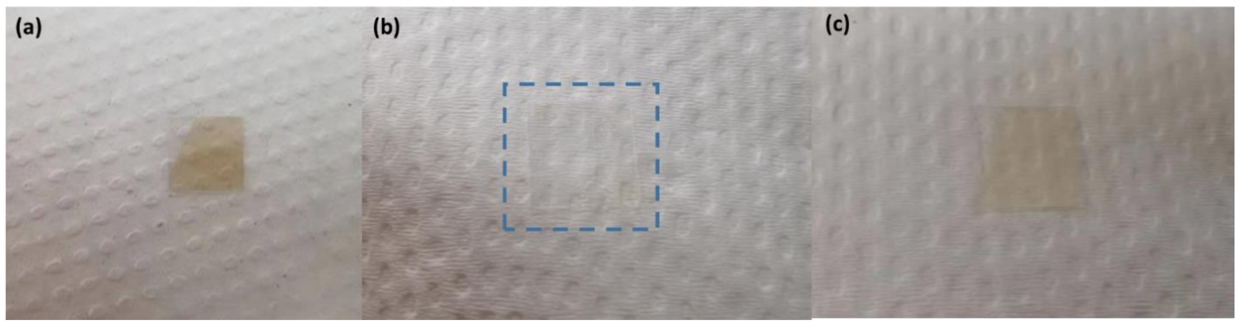

Supplementary Figure 1 **Optical image of BP sample on mica substrates** (a) after direct growth, (b) after wet transfer with EVA polymer in EG solvent and (c) after wet transfer with PS polymer in EG solvent.

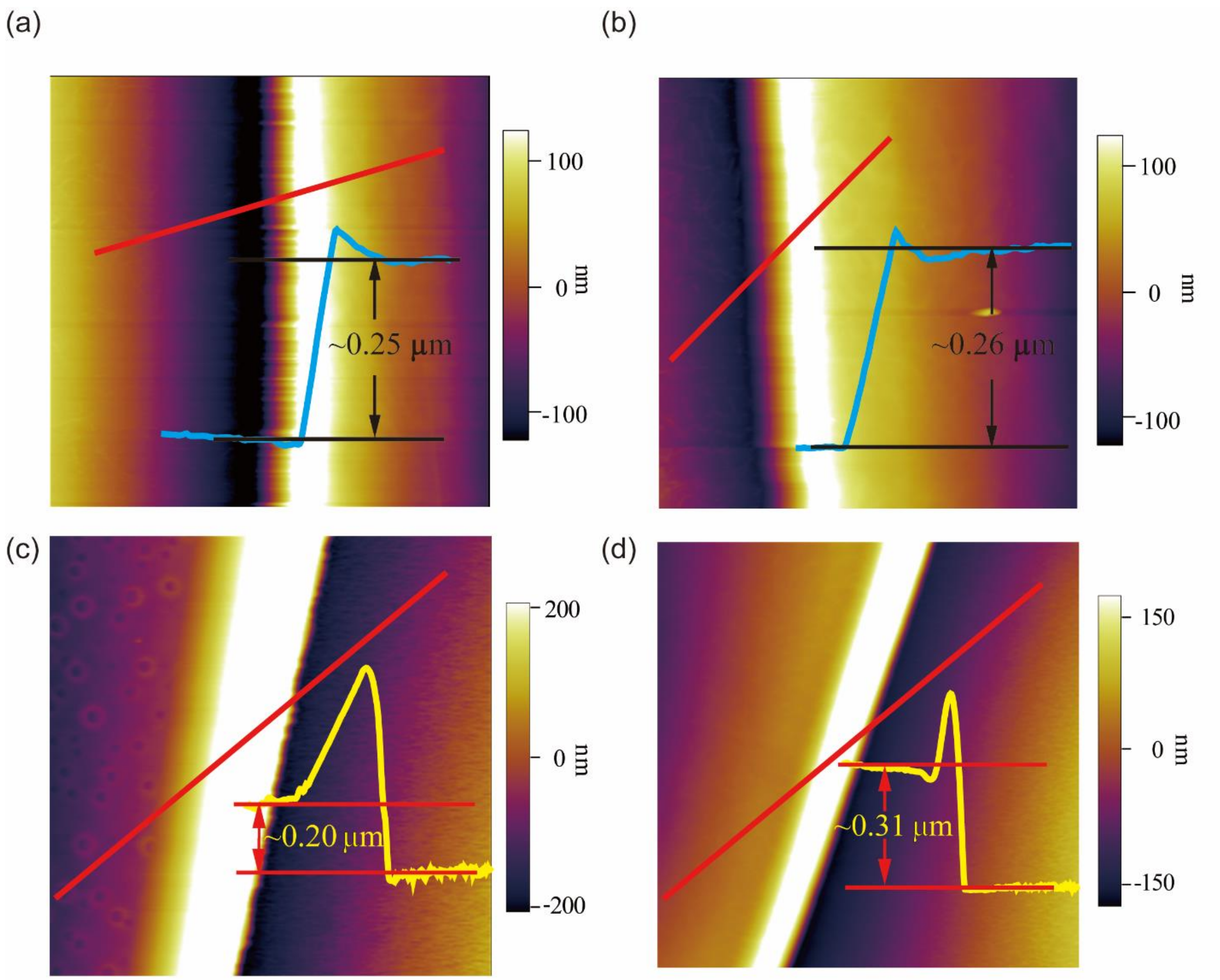

Supplementary Figure 2 **AFM topography and height analysis of the EVA polymer** (a) before and (b) after immersion in EG solvent. Similar analysis of the EVA polymer (c) before and (d) after immersion in IPA solvent.

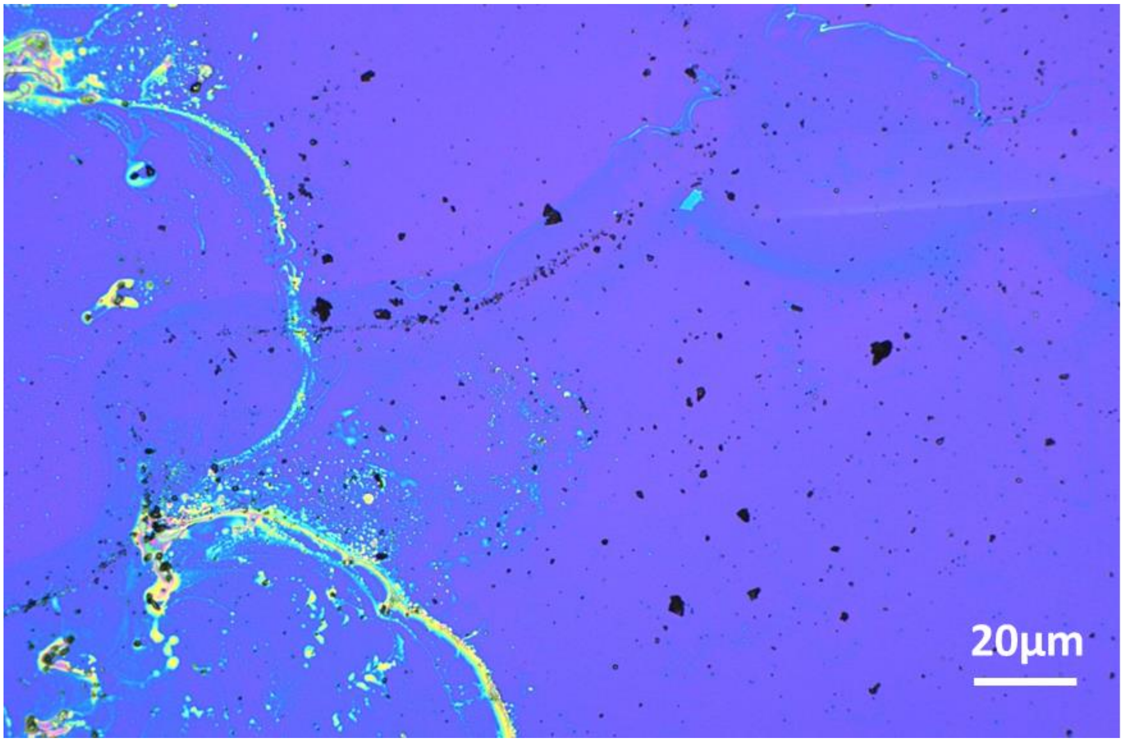

Supplementary Figure 3 Microscopic image of BP sample wet transferred on the SiO_2/Si substrate with PS polymer in EG solvent.

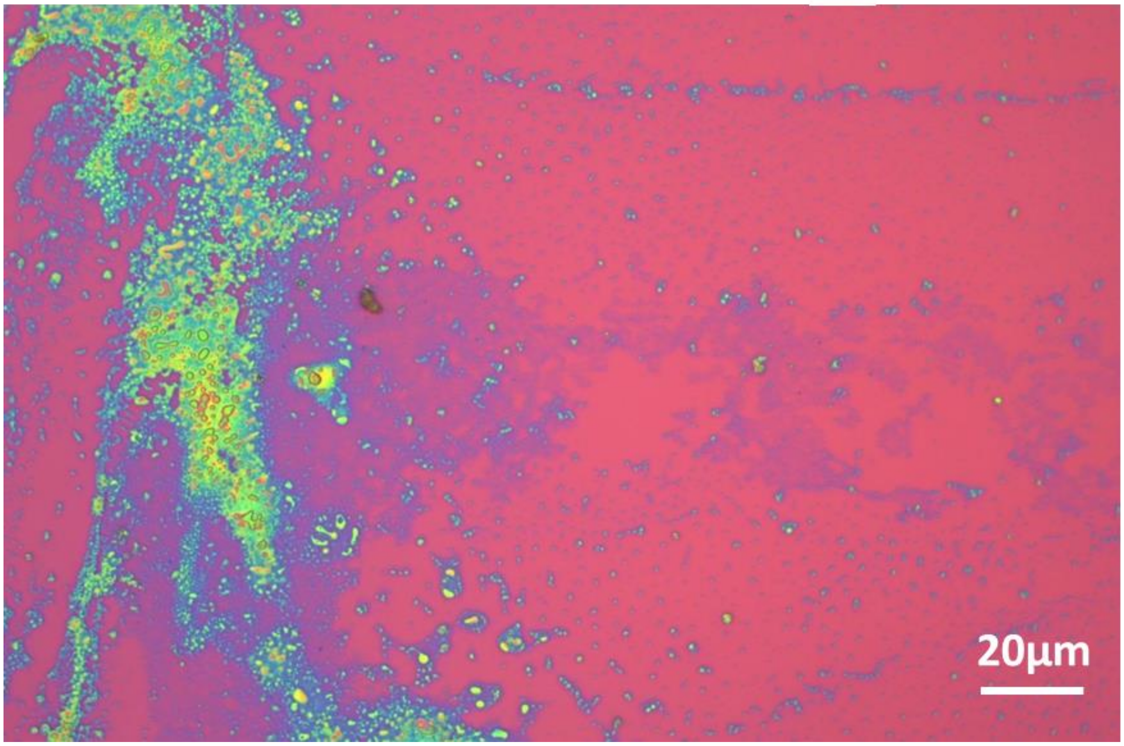

Supplementary Figure 4 Microscopic image of BP sample wet transferred on the SiO_2/Si substrate with EVA polymer in IPA solvent.

Supplementary Table 1 Surface energies of EG and glycerol utilized for the contact angle measurements (mN/m)

Tested liquid	**Total (Dispersion+Polarity)**	**Dispersion coefficient**	**Polarity coefficient**
EG	48	33.9	14.1
Glycerol	64	36.3	27.7

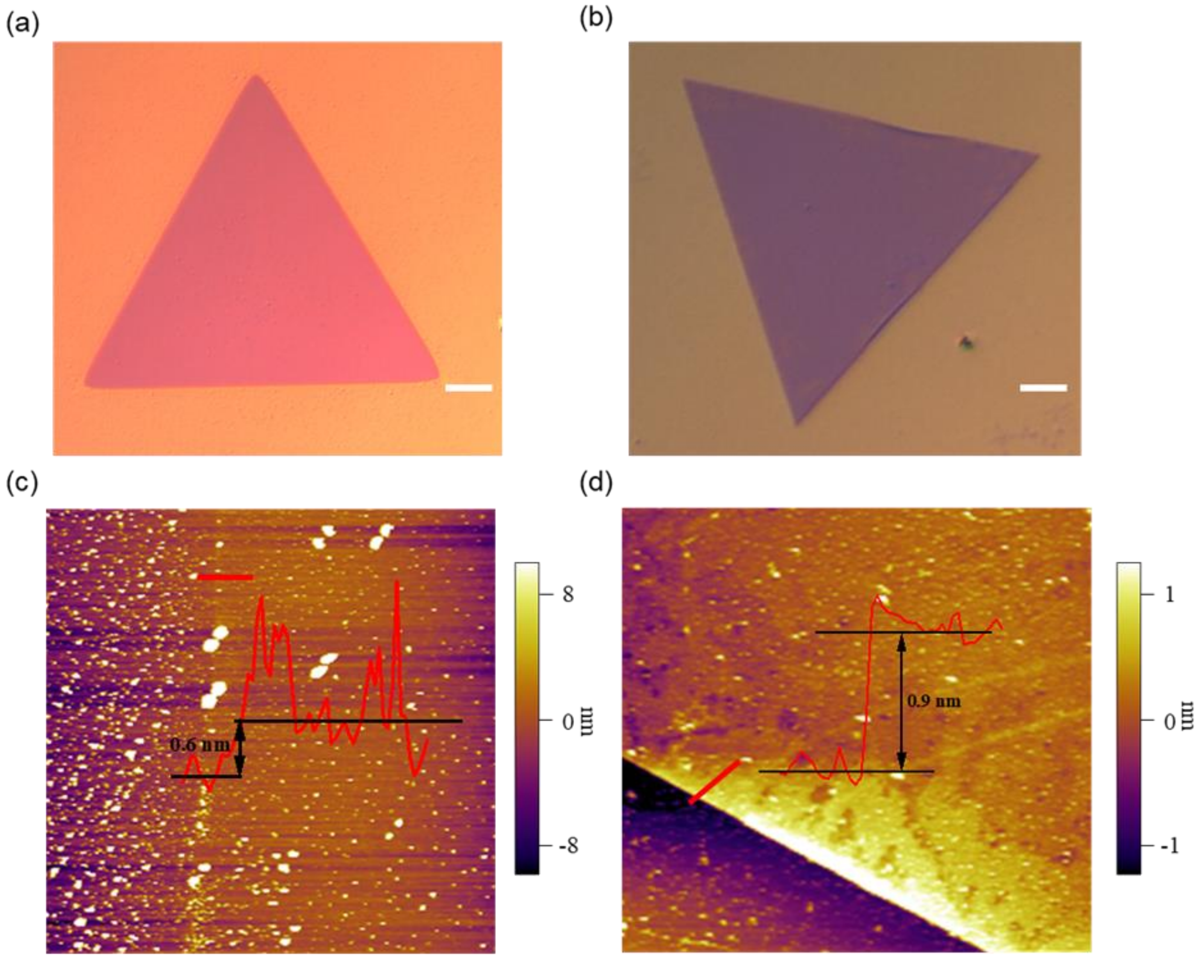

Supplementary Figure 5 **Surface topography of BP.** Microscopic image of (a) as-grown MoS_2 and (b) wet-transferred MoS_2. AFM images and height profiles of (c) direct grown and (d) wet-transferred MoS_2 thin films.

Our method is also expanded to the transfer of CVD-grown MoS_2 samples. Supplementary Figure 5 demonstrates that MoS_2 can be successfully transferred, resulting in a clean and high-quality surface without any detectable fractures.

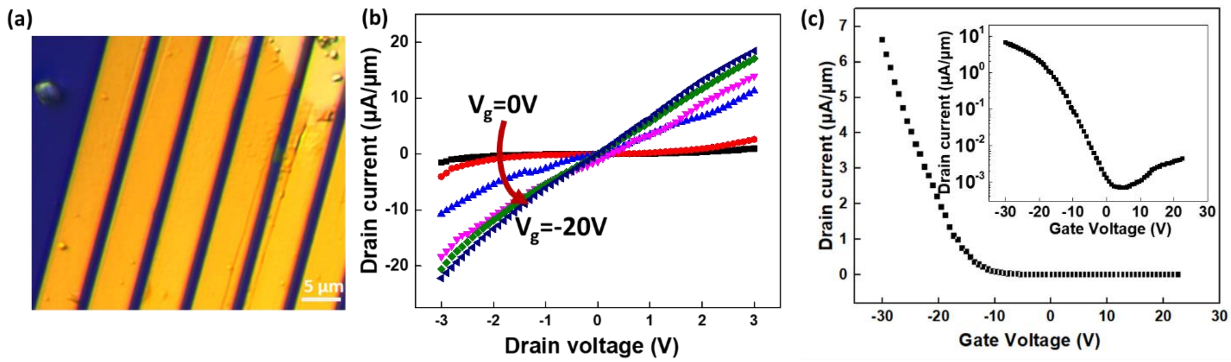

Supplementary Figure 6 **Transfer characteristics of BP FETs.** (a) Optical microscope image of BP FET arrays with 1 µm channel length on SiO_2/Si substrate. (b) I_{ds} -V_{ds} curves of the BP FET at V_g= 0 V, -1 V, -3 V, -5 V, -10 V, and -20 V. (c) Transfer characteristics of BP FET with 1 µm channel length in linear scale with -0.1 V drain voltage. Inset: Transfer characteristics in logarithmic scale.

BP FETs with a channel width of 1 µm were also fabricated, and the microscopic image of the device array is shown in Supplementary Figure 6a. Supplementary Figure 6b depicts the well-behaved I_{ds} –V_{ds} output characteristics of the FETs constructed using a BP thin film with a thickness of around 5 nm. The transfer characteristic is presented in Supplementary Figure 6c, while the field-effect mobility and on/off ratio of the BP FET was determined to be 312 $cm^2 V^{-1} s^{-1}$ and 7.8×10^3, respectively. This improved performance observed in BP FETs with a shorter channel length can be attributed to the fact that the back-gate electric field can more effectively modulate the charge carriers across the entire channel region. Also, in devices with longer channel, defects or non-uniformities in the BP film have a greater chance of propagating and affecting the entire channel and degrade the overall performance. In contrast, a shorter channel results in fewer potential defect sites, limiting the distance over which these defects can propagate and reducing their overall impact on device performance.